

Fig. 2 Temperature history of un-insulated surface.

approximation showed an error of 7.5%. The implicit Runge-Kutta deviated by only 0.5% from the explicit method (Fig. 2).

### Conclusion

The proposed method has been shown to be as accurate as the explicit Runge-Kutta. Unlike in the Runge-Kutta, the time increment is not dependent on the fineness of the mesh. In the example given, the implicit method was shown to execute four times faster than the explicit method with no significant difference in accuracy.

The implicit method combined with a Runge-Kutta integration on the surface conditions also has been shown to be significantly more accurate than the straight backward difference. In the example given there was no significant increase in execution time for the new method when using an equivalent compute interval.

The proposed method can be extended easily to composite materials and a variable mesh size. Also, the same method can be applied to the case with two exterior radiating surfaces. It should be possible to extend the method to two- and three-space dimensions by using a modification of the Douglas-Rachford method similar to that proposed by P.L.T. Brian.<sup>3</sup>

### References

<sup>1</sup> Gaumer, G. R., "Stability of Three Finite Difference Methods of Solving Transient Temperatures," *ARS Journal*, Vol. 32, No. 10, Oct. 1962, pp. 1595-1597.

<sup>2</sup> Richtmeyer, R. D. and Morton, K. W., *Difference Methods for Initial Value Problems*, 2nd ed., Interscience, New York, 1967, p. 189.

<sup>3</sup> Brian, P. L. T., "A Finite Difference Method of Higher-Order Accuracy for the Solution of Three-Dimensional Heat Conduction Problems," *A.I.Ch.E. Journal*, Vol. 7, No. 3, Sept. 1961, pp. 367-370.

## Some Plane Quadrilateral "Hybrid" Finite Elements

ROBERT D. COOK\* AND JAAFAR K. AL-ABDULLA†  
University of Wisconsin, Madison, Wis.

### Introduction

IN this Note the "hybrid" element of Pian<sup>1</sup> is generalized to arbitrary quadrilateral form. Four hybrids having constant and linear stress distributions are considered. An example problem is solved in order to compare the elements.

Received June 27, 1969. Thanks are expressed to the University Research Committee for providing computer time.

\* Associate Professor, Department of Engineering Mechanics.  
† Project Assistant, Mathematics Research Center.

Table 1 Matrix T for hybrids H1-H4

T	H1	H2	H3	H4	T	H1	H2	H3	H4
$T_{1,i}$	$a$	$a$	$a$	$a$	$T_{1,i+4}$	0	0	0	0
$T_{2,i}$	0	$c$	0	$e$	$T_{2,i+4}$	$b$	0	$b$	$-c$
$T_{3,i}$	$b$	0	$b$	$c$	$T_{3,i+4}$	$a$	$b$	$a$	0
$T_{4,i}$	...	0	$e$	0	$T_{4,i+4}$	...	$d$	$-c$	$b$
$T_{5,i}$	...	$b$	$-d$	0	$T_{5,i+4}$	...	$a$	$-e$	$d$
$T_{6,i}$	...	...	...	$-d$	$T_{6,i+4}$	...	...	...	$-e$
$T_{7,i}$	...	...	...	$b$	$T_{7,i+4}$	...	...	...	$a$

Hybrid elements considered are called  $H1$ ,  $H2$ ,  $H3$ , and  $H4$ . The notation of Pian<sup>1</sup> is used where possible. Thus  $\delta = P\beta$ , and the  $P$  matrices of the four hybrids are

$$H1 = \begin{bmatrix} 1 & 0 & 0 \\ 0 & 1 & 0 \\ 0 & 0 & 1 \end{bmatrix}, H2 = \begin{bmatrix} 1 & y & 0 & 0 & 0 \\ 0 & 0 & 1 & x & 0 \\ 0 & 0 & 0 & 0 & 1 \end{bmatrix}$$

$$H3 = \begin{bmatrix} 1 & 0 & 0 & x & 0 \\ 0 & 1 & 0 & 0 & y \\ 0 & 0 & 1 & -y & -x \end{bmatrix}$$

$$H4 = \begin{bmatrix} 1 & x & y & 0 & 0 & 0 & 0 \\ 0 & 0 & 0 & 1 & x & y & 0 \\ 0 & -y & 0 & 0 & 0 & -x & 1 \end{bmatrix}$$

### Formulation of Matrices

Consider an arbitrary quadrilateral of constant thickness  $t$  whose corners are numbered counterclockwise 1-4. Matrix  $T$  accounts for work done by boundary forces. Its form is determined by consideration of stress and displacement components in coordinate directions  $ns$ , where  $s$  coincides with the edge being treated, and the normal  $n$  makes a counterclockwise angle  $\theta$  with respect to the  $x$  axis (plate elements have been similarly treated; see, e.g., Ref. 2). The analysis is as follows. First, express  $ns$  nodal displacements, four for each edge, in terms of nodal displacements in  $xy$  coordinates,

$$\mathbf{q}' = \mathbf{W} \mathbf{q}, \quad W_{ij} = f_1(\theta) \quad (1)$$

Next, require that  $ns$  displacements along each edge be linear functions of  $s$ ,

$$\mathbf{u}' = \mathbf{L}' \mathbf{q}', \quad L_{ij}' = f_2(s, l) \quad (2)$$

where  $l$  is the length of an edge. Next, express  $ns$  edge stresses in terms of  $\beta$ ,

$$\mathbf{S} = \mathbf{Z} \mathbf{\delta} = \mathbf{Z} \mathbf{P} \beta, \quad Z_{ij} = f_3(\theta) \quad (3)$$

In  $\mathbf{P}$ , for example, along edge 1-2 we have  $x = x_1 - s \sin \theta_{12} = x_1 - s(x_1 - x_2)/l_{12}$ . Finally, matrix  $T$  results from integration of  $(\mathbf{Z} \mathbf{P})^T \mathbf{L}' \mathbf{W} = \mathbf{R}^T \mathbf{L}$  along the edges. Let

$$\begin{aligned} a &= t(y_k - y_i)/2, b = t(x_i - x_k)/2 \\ c &= t[y_k(y_j + y_k) - y_i(y_i + y_j)]/6 \\ d &= t[x_i(x_i + x_j) - x_k(x_j + x_k)]/6 \\ e &= t[y_j(x_k - x_i) + x_j(y_k - y_i) + 2(x_k y_k - x_i y_i)]/6 \end{aligned} \quad (4)$$

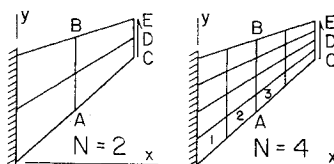
where  $i, j, k$  are cyclically permuted from 1-4 and  $i = j - 1$ .

Table 2 Times in milliseconds on CDC 3600 computer to form stiffness matrix and to compute and print stresses. Trace of stiffness matrix for square element with modulus  $E = 1.0$  and Poisson's ratio  $\nu = \frac{1}{3}$

Property	H1	H2	H3	H4	I1	I4	T4
Formation	17	60	60	92	16	50	110
Stresses	28 <sup>a</sup>	185	185	214	142	142	...
Trace	3.00	3.67	3.18	3.75	3.00	4.00	4.13

<sup>a</sup> Stresses at one point only.

Fig. 1 Arbitrary plane finite-element structure.



$k = j + 1$ . Thus, elements of  $\mathbf{T}$  for the hybrids may be listed as in Table 1.

Formation of matrix  $\mathbf{H}^{-1}$  is trivial for hybrid  $H1$ . For hybrids  $H2-H4$ , linear and quadratic terms must be integrated to produce  $\mathbf{H}$ ; this is done exactly by Gaussian quadrature using four integration points. Use was made of efficiencies suggested by Irons<sup>3</sup> for integration and manipulation of the form  $\mathbf{P}^T \mathbf{N} \mathbf{P}$ . Direct formation of  $\mathbf{H}$  using properties of plane areas should be faster, but lacks the generality desirable for further extension, e.g., to variable thickness elements.

Formation times for  $\mathbf{k}$  are given in Table 2. The trace of  $\mathbf{k}$  is given for subsequent reference. Also given in Table 2 is the time required for element stress computation, which consists of reforming  $\mathbf{H}^{-1} \mathbf{T}$ , postmultiplying by  $\mathbf{q}$ , premultiplying by  $\mathbf{P}$  for each element corner, and printing.

The grade 1 "isoparametric" quadrilateral<sup>3</sup> is a displacement model competitive with the hybrids. Data is given for this model in Table 2. Gaussian quadrature using one point ( $I1$ ) and four points ( $I4$ ) is considered (the latter is exact for a rectangular element). Finally Table 2 lists data for a quadrilateral composed of four constant-strain triangles ( $T4$ ).

#### Numerical Example and Conclusions

An arbitrary plane structure composed of nonrectangular elements (Fig. 1) was loaded by a uniformly distributed shear  $\tau_{xy}$  along edge CDE. Finite-element meshes of  $N = 1, 2, 4, 8$ , and 16 were used.

Vertical deflections of point D for the several meshes and elements are shown in Fig. 2. Validity of the hybrid formulations is confirmed by comparison with displacement models  $I1$  and  $I4$ . Results given by element  $T4$  are not shown, as they are practically identical to those given by element  $I4$ . Excluding  $T4$ , traces of nonrectangular elements are ranked in the same order seen in Table 2; hence, it appears that the quality of a  $\mathbf{k}$  matrix is not directly related to its trace, as has been suggested.<sup>4</sup> One-element structures not shown in Fig. 2 were kinematically unstable.

Stresses plotted in Fig. 3 are averages of stresses along AB in each pair of elements; e.g., along the lower quarter of AB the plotted stress represents  $[(\sigma_x \text{ in el. } 2)_{AB} + (\sigma_x \text{ in el. } 3)_{AB}]/2$ .

Formulations  $H1$  and  $I1$  produce identical stiffness matrices, regardless of element shape. Stresses calculated by use of  $I1$  are unsatisfactory in a coarse mesh, even though the calculation of stresses from displacements involves no numerical integration; however (as expected<sup>3</sup>)  $I1$  is satisfactory in a fine mesh. Hybrid  $H1$  seems preferable to both  $I1$  and  $I4$ . Hybrid  $H2$  seems preferable to  $I4$  in spite of the time disadvantage seen in Table 2. The additional stress modes in  $H3$  and  $H4$  produce no advantage over  $H2$ , a conclusion in agreement with remarks of Pian and Tong.<sup>5</sup>

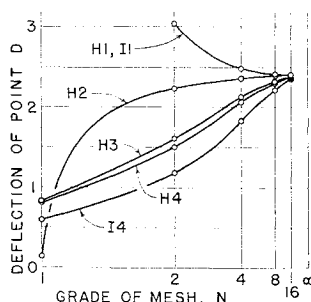
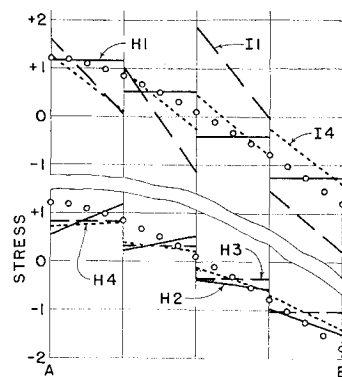


Fig. 2 Vertical deflection of point D in Fig. 1.

Fig. 3 Stress  $\sigma_x$  along line AB in Fig. 1 for  $N = 4$ . Circles represent node point averages for  $N = 16$  produced by hybrid  $H4$ .



#### References

<sup>1</sup> Pian, T. H. H., "Derivation of Element Stiffness Matrices by Assumed Stress Distributions," *AIAA Journal*, Vol. 2, No. 7, July 1964, pp. 1333-1336.

<sup>2</sup> Dungar, R. and Severn, R. T., "Triangular Finite Elements of Variable Thickness and Their Application to Plate and Shell Problems," *Journal of Strain Analysis*, Vol. 4, No. 1, Jan. 1969, pp. 10-21.

<sup>3</sup> Irons, B. M., "Engineering Applications of Numerical Integration in Stiffness Methods," *AIAA Journal*, Vol. 4, No. 11, Nov. 1966, pp. 2035-2037.

<sup>4</sup> Khanna, J., "Criterion for Selecting Stiffness Matrices," *AIAA Journal*, Vol. 3, No. 10, Oct. 1965, p. 1976.

<sup>5</sup> Pian, T. H. H. and Tong, P., "Rationalization in Deriving Element Stiffness Matrix by Assumed Stress Approach," presented at Second Conference on Matrix Methods in Structural Mechanics, Wright-Patterson Air Force Base, Ohio, Oct. 1968.

## An Experimental Investigation of the Buckling of Toroidal Shells

B. O. ALMROTH,\* L. H. SOBEL,† AND A. R. HUNTER‡  
Lockheed Missiles & Space Company, Palo Alto, Calif.

#### Nomenclature

<i>a</i>	= meridional radius of curvature (see Fig. 1)
<i>b</i>	= distance between the center of the circular meridian and the axis of revolution (see Fig. 1)
<i>E</i>	= Young's modulus
<i>h</i>	= thickness of shell
<i>p</i>	= uniform hydrostatic pressure loading

**T**HEORETICAL results for the buckling of toroidal shells under uniform external pressure are presented by Sobel and Flügge.<sup>1</sup> These results are in very good agreement with the few available test results. However, these experimental results are for a rather slender torus ( $b/a = 8$ , see Fig. 1 for notation). Therefore toroidal shells with a smaller value of  $b/a$  were manufactured and tested. The dimensions of the tested shells are  $b = 5$  in.,  $a = 2.5$  in., and thickness  $h = 0.050$  in. For a meaningful comparison between theory and test, it is important that the test specimen has a reasonably uniform thickness distribution. It was believed that this could best be achieved if the shells are manufactured by casting an epoxy resin material. The toroidal shell was cast in two halves which were later glued together. In this way excess-

Received June 13, 1969. This research was supported by the Independent Research Program of Lockheed Missiles & Space Company.

\* Senior Staff Scientist, Aerospace Sciences Laboratory. Member AIAA.

† Research Scientist, Aerospace Sciences Laboratory. Member AIAA.

‡ Research Scientist, Aerospace Sciences Laboratory.